Nucleotide Hydrolysis and Protein Conformational Changes in *Azotobacter vinelandii* Nitrogenase Iron Protein: Defining the Function of Aspartate 129[†]

William N. Lanzilotta, Matthew J. Ryle, and Lance C. Seefeldt*

Department of Chemistry and Biochemistry, Utah State University, Logan, Utah 84322

Received May 9, 1995; Revised Manuscript Received June 27, 1995[⊗]

ABSTRACT: The biological reduction of dinitrogen catalyzed by nitrogenase requires the hydrolysis of a minimum of 16 MgATP for each N_2 reduced. The present work examines the role of a strictly conserved aspartic acid residue of nitrogenase iron protein (Fe protein) in coupling MgATP hydrolysis to electron transfer and substrate reduction. The aspartic acid residue at position 129 in the *Azotobacter vinelandii* Fe protein has been suggested to participate in nucleotide interactions from its location in the X-ray structure near several amino acids previously identified to participate in nucleotide binding and protein conformational changes. The function of this amino acid was probed by changing aspartic acid to glutamic acid (D129E) and asparagine (D129N) by site-directed mutagenesis. The D129N Fe protein proved to be unstable and could not be purified. Characterization of the purified D129E Fe protein revealed a central role for Asp 129 in the nucleotide-induced protein conformational changes in the Fe protein and possibly in the mechanism of MgATP hydrolysis. Data from EPR, circular dichroism spectroscopy, and Fe^{2+} chelation rates and the chemical shifts of isotropically shifted protons in the ^1H NMR spectra implicate Asp 129 in the nucleotide-induced conformational changes in the Fe protein, which are reflected in changes in the environment of the [4Fe-4S] cluster. The D129E Fe protein was found to bind both MgATP and MgADP with high affinity. The K_d determined for MgADP binding (K_d = 131 μM) was comparable to that found for wild-type Fe protein (128 μM). The affinity for MgATP binding was 1.6 times tighter than that for wild-type Fe protein (370 compared to 580 μM). The midpoint reduction potential of the [4Fe-4S] cluster was similar to that determined for the wild-type Fe protein (−290 mV for wild-type Fe protein and −300 mV for D129E Fe protein). Upon the addition of MgATP or MgADP, the midpoint potentials for wild-type and D129E Fe proteins shifted to −430 and −440 mV, respectively. The D129E Fe protein was also found to bind to the molybdenum−iron protein (MoFe protein) with normal affinity, although it could not support electron transfer to the MoFe protein or MoFe protein-stimulated MgATP hydrolysis.

The biological reduction of dinitrogen is catalyzed by the two-component metalloenzyme, nitrogenase, according to the following overall reaction:

$$N_2 + 8H^+ + 16MgATP + 8e^- \rightarrow 2NH_3 + H_2 + 16MgADP + 16P_i \quad (1)$$

A detailed description of the function of MgATP hydrolysis in the nitrogenase substrate reduction mechanism has yet to emerge (Burris, 1991; Smith & Eady, 1992; Dean et al., 1993; Mortenson et al., 1993; Howard & Rees, 1994; Kim & Rees, 1994). The current model suggests that MgATP hydrolysis is coupled to the transfer of electrons from the nitrogenase iron protein (Fe protein)[1] to the molybdenum−iron protein (MoFe protein), and possibly directly to substrate reduction. The MoFe protein is an $\alpha_2\beta_2$ tetramer which contains two molybdenum−iron−sulfur−homocitrate metal clusters (FeMoco) (Kim & Rees, 1992) and two [8Fe-(7−8)S] clusters (P or 8Fe clusters) (Bolin et al., 1990; Kim et al., 1993). FeMoco is thought to be the site of substrate binding and reduction and the 8Fe clusters appear to mediate electron transfer from the Fe protein to the FeMoco (Lowe et al., 1993). The Fe protein is a homodimeric protein with a single [4Fe-4S] cluster bound between its subunits (Georgiadis et al., 1992). Each subunit of the Fe protein also contains a nucleotide-binding site, which is located approximately 19 Å from the [4Fe-4S] cluster. During catalysis, the reduced Fe protein, with two MgATPs bound, binds to the MoFe protein. The MgATPs are hydrolyzed and a single electron is transferred from the Fe protein to the MoFe protein (possibly the 8Fe cluster). The oxidized Fe protein, with two bound MgADPs, is released from the MoFe protein in the reaction rate-limiting step (Hageman & Burris, 1978; Thorneley & Lowe, 1985). Another reduced Fe protein, with two bound MgATPs, binds to the partially reduced MoFe protein for a second round of MgATP hydrolysis and electron transfer. This cycle is repeated until sufficient electrons have been transferred to the MoFe protein to reduce the substrate. The released Fe $protein_{ox}$−$(MgADP)_2$ complex is reduced by low-potential electron transfer proteins (e.g., flavodoxin or ferredoxin), and the MgADP is replaced by MgATP.

[†] This work was supported by National Science Foundation Grant MCB-9315835.

* Author to whom correspondence should be addressed: phone, (801) 797-3964; Fax, (801) 797-3390; internet, seefeldt@cc.usu.edu.

[⊗] Abstract published in *Advance ACS Abstracts,* August 15, 1995.

[1] Abbreviations: Fe protein, iron protein of nitrogenase; MoFe protein, molybdenum−iron protein of nitrogenase, $Fe\ protein_{ox}$, oxidized iron protein of nitrogenase; $Fe\ protein_r$, reduced iron protein of nitrogenase; FeMoco, iron−molybdenum cofactor; EPR, electron paramagnetic resonance; CD, circular dichroism; *Av2*, *Azotobacter vinelandii* Fe protein; *Cp2*, *Clostridium pasteurianum* Fe protein; ^1H NMR, proton nuclear magnetic resonance spectroscopy; MOPS, 3-morpholinopropanesulfonic acid; BPS, bathophenanthrolinedisulfonic acid; Tris, tris(hydroxymethyl)aminomethane; IDS, indigo disulfonate.

0006-2960/95/0434-10713$09.00/0

The Fe protein can bind two MgATPs per protein, and this binding is known to induce protein conformational changes that are reflected in changes in the environment of the [4Fe-4S] cluster (Zumft et al., 1972; Stephens et al., 1979; Watt et al., 1986; Meyer et al., 1988; Seefeldt et al., 1992). It is clear that the binding of MgATP to the Fe protein and the resulting conformational changes are a prerequisite for Fe protein docking to the MoFe protein prior to catalysis. Another consequence of nucleotide binding to the Fe protein is the lowering of the midpoint potential of the Fe protein [4Fe-4S] cluster by over −100 mV. It has been stated that this lowering of the reduction potential is one of the driving forces for electron transfer from the Fe protein to the MoFe protein. Once bound to the MoFe protein, the Fe protein−MgATP complex becomes competent for MgATP hydrolysis and reduction of the MoFe protein. The Fe protein is the only known reductant that can support substrate reduction on the MoFe protein, clearly suggesting functions other than simple reduction of the MoFe protein.

As one way to begin to define both the site of nucleotide binding on the Fe protein and the mechanism of coupling nucleotide hydrolysis to intercomponent electron transfer, we are defining the function of specific amino acids within the Fe protein by site-directed mutagenesis and characterization of the altered proteins. Earlier studies have identified several amino acids within the Fe protein that are involved in nucleotide interactions, including interactions with the phosphate and Mg^{2+} portions of bound nucleotides. All nitrogenase Fe proteins for which sequences are available contain a consensus amino acid sequence (P-loop or Walker A) often associated with nucleotide-binding proteins (Normand & Bousquet, 1989). Two residues within this conserved P-loop have been demonstrated to function in nucleotide binding. Specifically, Lys 15 of *Azotobacter vinelandii* Fe protein was found to function in the binding of nucleotides (Seefeldt et al., 1992; Ryle et al., 1995), and the adjacent Ser 16 was found to interact with Mg^{2+} associated with the bound nucleotide (Seefeldt & Mortenson, 1993). The assignment of the probable functions of these amino acids was supported by analysis of the X-ray structure of the Fe protein and the location of an adventitiously bound ADP molecule in the structure (Georgiadis et al., 1992). Recent evidence from the analysis of the properties of an Fe protein in which Asp 125 was altered to Glu demonstrated that this residue was involved in interactions with the bound nucleotide and played a central role in communication from the nucleotide-binding site to changes in the [4Fe-4S] cluster, possibly mediated through changes in Cys 132, a ligand to the [4Fe-4S] cluster (Wolle et al., 1992).

Analysis of the X-ray structure of the Fe protein, coupled with knowledge of the functions of Asp 125, Lys 15, and Ser 16, suggested that Asp 129 might be involved in nucleotide interactions with Fe protein. Three possible functions were suggested: (1) direct involvement in nucleotide binding, (2) a role in the communication pathway between the nucleotide-binding site and the [4Fe-4S] cluster, and (3) a possible catalytic role in MgATP hydrolysis. To probe these possible functions, Asp 129 of the *A. vinelandii* Fe protein was changed to the amino acids glutamate (D129E) and asparagine (D129N), and the properties of the altered Fe proteins were characterized. The results presented in this work demonstrate that Asp 129 is involved in communication between the [4Fe-4S] cluster and the nucleotide-binding site and, possibly, in MgATP hydrolysis. Finally, data are presented suggesting that the lowering of the midpoint potential of the [4Fe-4S] cluster of the Fe protein is not sufficient for electron transfer to the MoFe protein, but that the hydrolysis of MgATP is an absolute requirement.

EXPERIMENTAL PROCEDURES

Site-Directed Mutagenesis, Expression, and Purification of Altered and Wild-Type Fe Proteins. Site-directed mutagenesis of the nitrogenase Fe protein gene from *A. vinelandii*, *nif H*, was performed as previously described (Jacobson et al., 1989a,b; Seefeldt & Mortenson, 1993). The altered Fe protein was expressed in *A. vinelandii* and purified to homogeneity also as previously described (Seefeldt & Mortenson, 1993). Protein concentrations were determined by a modified Biuret method (Chromy et al., 1974), with bovine serum albumin as the standard. All proteins used were homogeneous as determined by analysis on SDS gels with Coomassie staining (Seefeldt et al., 1992). All protein manipulations were done in the absence of oxygen under an atmosphere of argon. All buffers used were saturated with argon and contained 2 mM sodium dithionite ($Na_2S_2O_4$), unless noted otherwise.

Activity Assays and MgATP Hydrolysis. Acetylene and proton reduction rates were determined with 10 mM dithionite as the reductant as previously described (Seefeldt et al., 1992; Seefeldt & Mortenson, 1993), except that the buffer was 100 mM MOPS (pH 7.0). MgATP hydrolysis rates were determined in assay solution without the MgATP-regenerating system. MgADP formed during the assay was quantified by the HPLC method previously described (Seefeldt, 1994). The stoichiometry of MgATP hydrolyzed per electron transferred was determined from the rates of electron transfer to substrates and the rates of MgATP hydrolysis, as previously described (Seefeldt, 1994).

Equilibrium MgATP and MgADP Binding to Fe Protein. The binding of MgATP or MgADP to the wild-type and D129E Fe proteins was determined by the equilibrium column technique previously described (Ryle et al., 1995). A Sephadex G-25 column (0.7 × 10 cm) was equilibrated with 50 mM Tris buffer (pH 8.0) containing 2 mM dithionite and different concentrations of MgATP (0−1500 μM) or MgADP (0−300 μM). The columns were developed following the addition of 3.6 mg (56 nmol) of the Fe protein. Fractions were analyzed for protein by the modified Biuret method (Chromy et al., 1974) and for nucleotide concentration by the HPLC method previously described (Seefeldt & Mortenson, 1993).

MgATP-Dependent Fe^{2+} Chelation from Wild-Type and D129E Fe Proteins. The MgATP-dependent chelation of Fe^{2+} from the Fe protein was followed continuously by the formation of the Fe^{2+}−α,α′-bipyridyl complex, which was monitored spectrophotometrically at 520 nm by using an absorption coefficient of 8400 M^{-1} cm^{-1} (Walker & Mortenson, 1974; Seefeldt et al., 1992). All reactions were carried out in 2 mL sealed cuvettes under an atmosphere of argon, with a total liquid volume of 1 mL. The chelation assay solution consisted of 35 mM Tris buffer (pH 8.0) with 6.25 mM α,α′-bipyridyl and 1.3 mM dithionite. The reaction was initiated by the addition of the indicated quantity of Fe protein. All spectrophotometric measurements were done

on a Hewlett-Packard 8452A diode array spectrophotometer interfaced to a computer for data acquisition. MgATP was added at the indicated time to a final concentration of 3.9 mM.

The MgATP-dependent chelation of Fe^{2+} from Fe protein was also determined with the chelator bathophenanthrolinedisulfonic acid (BPS). The formation of the Fe^{2+}−BPS complex was monitored spectrophotometrically at 534 nm by using an absorption coefficient of 22 140 M^{-1} cm^{-1} (Ljones & Burris, 1978). The chelation assay solution consisted of 44 mM Tris buffer (pH 8.0) with 1.1 mM BPS and 2 mM dithionite. Reactions were initiated by the addition of 345 μg (5.3 nmol) of Fe protein. MgATP was added approximately 60 s later to a final concentration of 3.9 mM.

To determine the potential for Fe protein binding to MoFe protein, the effects of the addition of MoFe protein on the rate of Fe^{2+} chelation from the Fe protein in both the α,α'-bipyridyl and BPS chelation assays were determined. In these assays, 6 mM creatine phosphate and 0.125 mg/mL creatine phosphokinase were included to prevent any MgADP formation. The indicated quantity of MoFe protein was added to the assay vials prior to the introduction of the Fe protein. MgATP was added at the indicated times.

Midpoint Reduction Potential of the [4Fe-4S] Cluster in Wild-Type and D129E Fe Protein. The midpoint reduction potentials for the $[4Fe\text{-}4S]^{2+}/[4Fe\text{-}4S]^{1+}$ couple in wild-type and D129E Fe proteins were determined by microcoulometry as previously described (Ryle et al., 1995). The reduced Fe protein was oxidized in an argon-filled glove box by adding 5.6 mM indigo disulfonate until a blue color remained. The oxidized Fe protein was then passed through a Sephadex G-25 column (0.7 × 10 cm) equilibrated with a 50 mM Tris buffer (pH 8.0) under argon to remove the small molecules. The concentration of oxidized Fe protein was determined from absorbance at 400 nm by using an extinction coefficient of 13.3 mM^{-1} cm^{-1}(Anderson & Howard, 1984). Electrochemical reductions were determined from 150 μg aliquots of oxidized Fe protein in 50 mM Tris buffer (pH 8.0) with 200 mM NaCl, 0.1 mM methyl viologen, 0.1 mM benzyl viologen, and 0.1 mM flavin mononucleotide. Midpoint reduction potentials in the presence of nucleotides were determined by adding either MgATP or MgADP to a final concentration of 3 mM in the assay solution. The fraction of Fe protein in the reduced state was plotted against the applied potential over a range of −150 to −450 mV in 30 mV increments. The data were fit to the Nernst equation to determine the midpoint potential, and all potentials were relative to the standard hydrogen electrode (SHE).

EPR. EPR spectra of the dithionite-reduced state of Fe protein were recorded at 12 K as previously described (Seefeldt et al., 1992). Where indicated, MgATP was added to a 10-fold molar excess over protein from a stock solution prior to freezing. All spectra were recorded on a Bruker ER300E spectrometer with an Air Products liquid helium cryostat.

Circular Dichroism Spectra of Fe Protein Samples with or without Nucleotides. Twenty milligrams (312 nmol) of Fe protein containing 2 mM dithionite was desalted on a Sephadex G-25 column (0.5 × 10 cm) equilibrated with 100 mM Tris buffer (pH 8.0) without dithionite. The Fe protein was then oxidized by the addition of 20 μL of a 20 mM indigo disulfonate (IDS) solution. IDS was removed from the oxidized Fe protein by passage through a Dowex 1 column (1.0 × 5 cm) equilibrated with anaerobic 100 mM Tris buffer (pH 8.0). The oxidized Fe protein was split equally into two 4 mL sealed quartz cuvettes under an argon atmosphere. The total volume of each cuvette was brought to 2 mL by the addition of 100 mM Tris buffer (pH 8.0). Where indicated, nucleotides (MgATP or MgADP) were added to a final concentration of 1 mM. All spectra were recorded by using an Aviv model 62DS spectropolarimeter and were baseline corrected.

^1H NMR Spectra of the Isotropically Shifted Protons Observed for the Wild-Type and D129E Fe Proteins. Fe protein samples for NMR were exchanged into a Tris-buffered D_2O solution (140 mg of Tris·HCl and 40 mg of Tris base in 20 mL of D_2O with 5 mM dithionite) by passage through a Sephadex G-25 column. When H_2O was used to dissolve these components, the pH was found to be 7.7, so the pD of the deuterated buffer was not measured. The proteins were concentrated with a Centricon 30 (Amicon Division, Beverly, MA) to 35−45 mg mL^{-1}. In all cases, anaerobic glass (5 mm) NMR tubes were used (Wilmad, Buena, NJ). ^1H NMR spectra were carried out on a Bruker 400 MHz spectrometer by using the modified DEFT pulse sequence (Hochmann & Kellerhals, 1990) to suppress the water signal and diamagnetic protons of the protein. A total of 5000 scans was taken with 8000 data points and a sweep width of 200 ppm. The total experiment time was 38 min at 313 K. All chemical shifts were referenced to the water proton signal at 4.7 ppm. A 30 Hz line broadening was introduced to improve the signal to noise ratio. Nucleotides were added to a final concentration of 5 mM. Recovery of wild-type Fe protein samples following NMR experiments showed less than a 5% loss in activity.

Titanium(III) Citrate-Coupled Spectrophotometric Assays of Electron Utilization by the Fe Proteins. The flow of electrons through the nitrogenase Fe protein was monitored by following the oxidation of Titanium(III) citrate during turnover conditions as previously described (Seefeldt & Ensign, 1994). Conditions were similar to the proton reduction assay, except that the reaction was carried out in 2 mL quartz cuvettes in the absence of dithionite. A sample of 12.3 μL of an 83 mM Titanium(III) citrate solution was added to the cuvette to initiate the reaction. The oxidation of Titanium(III) citrate by the Fe protein was monitored at 340 nm, with the absorption coefficient taken to be 0.73 mM^{-1} cm^{-1} (Seefeldt & Ensign, 1994).

Binding of D129E Fe Protein to the MoFe Protein. To test the possibility that the D129E Fe protein could still bind to the MoFe protein, a competition assay was developed. In this assay, increasing quantities of the D129E Fe protein were added to fixed quantities of wild-type Fe protein (1.8 nmol) and MoFe protein (0.9 nmol) and the effects of added D129E Fe protein on acetylene reduction rates were determined. From a plot of the percent of maximal wild-type activity versus the ratio of D129E Fe protein to wild-type Fe protein, the ability of the D129E Fe protein to bind to the MoFe protein was quantified. A K15R Fe protein, which has previously been shown not to bind to the MoFe protein, was used as a negative control (Ryle et al., 1995).

RESULTS

Changing Asp 129 of the A. vinelandii Fe Protein by Site-Directed Mutagenesis. Analysis of the *A. vinelandii* Fe

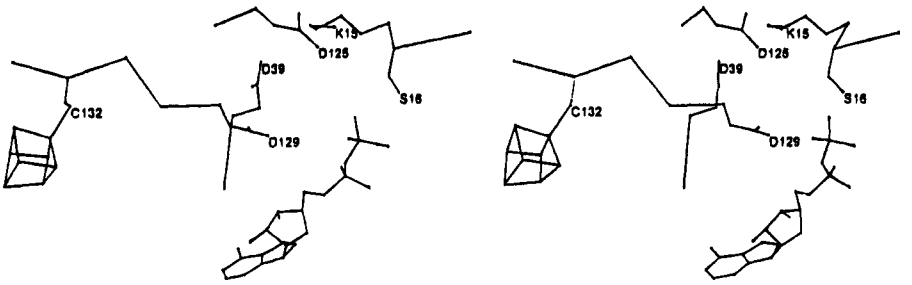

FIGURE 1: Stereoscopic view of the *A. vinelandii* Fe protein nucleotide phosphate-binding site. The model presents the positions of the [4Fe-4S] cluster (cubane structure), ADP (lower right), and the side chains of the amino acids Lys 15 (K15), Asp 125 (D125), Ser 16 (S16), Asp 39 (D39), and Asp 129 (D129). The α-carbon backbone trace is shown from Asp 129 to Cys 132, a ligand to the [4Fe-4S] cluster.

protein X-ray crystal structure suggests that Asp 129, a strictly conserved amino acid among all known Fe proteins, might serve three possible functions in nucleotide interactions with the Fe protein (Figure 1). First, the relative position of Asp 129 to the three amino acid residues previously shown to be involved in nucleotide binding (Asp 125, Lys 15, and Ser 16) suggested that Asp 129 might participate in the binding of nucleotides through interaction with Mg^{2+} or a bound water. Similarly, Asp 129 may serve a catalytic role in the hydrolysis of MgATP. Finally, the location of Asp 129 between Asp 125 and Cys 132 suggested a possible role in the communication between the nucleotide-binding site and the [4Fe-4S] cluster. Asp 125 has been shown to interact with bound nucleotide (possibly bound Mg^{2+} or a bound water) and Cys 132, a ligand to the [4Fe-4S] cluster (Wolle et al., 1992).

To investigate these possible roles for Asp 129 in nitrogenase function, this residue was changed by site-directed mutagenesis to the amino acids glutamate (D129E) and asparagine (D129N). Changing aspartic acid to glutamic acid provides a conservative amino acid change while maintaining the carboxylate side chain. Changing Asp to Asn would remove the negatively charged carboxylate side chain and is predicted to be a conservative structural change (Bordo & Argos, 1991). The altered Fe proteins (D129E and D129N) were expressed in *A. vinelandii* cells in place of the wild-type Fe protein. This was accomplished by replacing the chromosomal wild-type Fe protein gene, *nif H*, with the mutated gene by a homologous recombination procedure (Jacobson et al., 1989a,b). The *A. vinelandii* cells expressing the altered Fe protein were tested for their ability to grow under nitrogen-fixing conditions to analyze the functional consequences of the amino acid changes. *A. vinelandii* cells expressing either the D129E- or D129N-altered Fe proteins were unable to grow under nitrogen-fixing conditions, revealing that changing Asp 129 to Glu or Asn renders the Fe protein inactive in nitrogen fixation. It was of interest to investigate the properties of the purified, altered Fe proteins to further define the functional consequences of the amino acid change and, thus, the function of Asp 129. The D129E and D129N Fe proteins were overexpressed in *A. vinelandii* cells using a derepression protocol previously described (Seefeldt et al., 1992). The D129N Fe protein could not be purified, probably reflecting instability in the altered Fe protein. In contrast, the D129E Fe protein could be purified to homogeneity in yields averaging 145% of wild-type Fe protein yields. The higher yields associated with the D129E could be indicative of greater stability. The properties of the purified D129E Fe protein were investigated further.

Activities of the D129E and Wild-Type Fe Proteins. The wild-type Fe protein−MoFe protein complex was found to reduce acetylene at a maximum rate of 1827 nmol of C_2H_4 evolved min^{-1} (mg of Fe protein)$^{-1}$ and protons at a maximum rate of 1880 nmol of H_2 evolved min^{-1} (mg of Fe protein)$^{-1}$. The D129E Fe protein, when combined with wild-type MoFe protein, did not support any detectable reduction in acetylene or protons. The wild-type Fe protein−MoFe protein complex was found to hydrolyze MgATP at a rate of 8120 nmol of MgADP formed min^{-1} (mg of Fe protein)$^{-1}$, with a stoichiometry of 2.5 ± 0.1 MgATP hydrolyzed per electron transferred. Even after the assay time was doubled, no MgATP hydrolysis could be detected for the D129E Fe protein−MoFe protein complex. As another way to monitor the flow of electrons through nitrogenase, the rate of oxidation of the reductant Titanium-(III) citrate was monitored spectrophotometrically (Seefeldt & Ensign, 1994). In this assay, no oxidation of Titanium-(III) citrate by the D129E Fe protein−MoFe protein complex was observed, while the wild-type Fe protein−MoFe protein complex had a maximum rate of 3931 nmol of electrons transferred min^{-1} mg^{-1}. These results reveal that changing Asp 129 to Glu results in an Fe protein that is unable to support electron transfer to the MoFe protein or MgATP hydrolysis.

Nucleotide Binding to the D129E and Wild-Type Fe Proteins. Since the D129E Fe protein could not support substrate reduction or MgATP hydrolysis, it was important to determine whether the lack of nucleotide hydrolysis was the result of a decreased affinity for nucleotide binding. MgATP and MgADP bind to the wild-type Fe protein as rapid equilibrium substrates with a maximum stoichiometry of two nucleotides per protein. The equilibrium dissociation constants (K_d) for MgATP and MgADP binding to reduced wild-type Fe protein have been determined by a variety of techniques and range from 17 to 1710 μM for MgATP and from 5 to 91 μM for MgADP (Yates, 1991). We determined the affinity for nucleotide binding for both the wild-type and D129E Fe proteins by using a modified equilibrium column technique (Ryle et al., 1995). In this technique, the Fe protein was passed through a G-25 column equilibrated with buffer containing a known concentration of MgATP or MgADP. A sample was then collected as the protein eluted from the column, and the concentrations of protein and nucleotide were determined. Figure 2 illustrates typical binding curves determined for wild-type and D129E Fe proteins by this technique. As can be seen, changing Asp 129 to Glu had no significant effect on the affinity for binding MgADP (apparent K_d for the D129E Fe protein was 131 μM and that for the wild-type Fe protein was 128 μM).

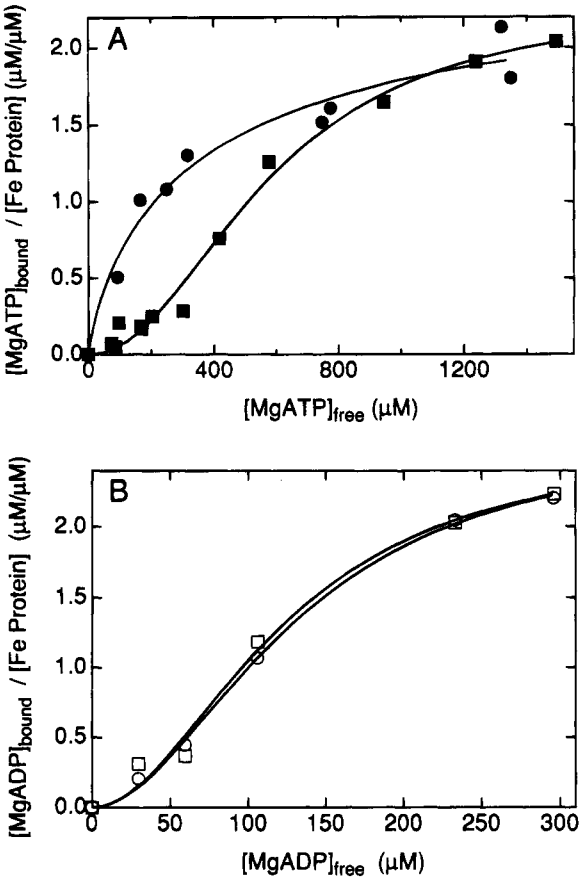

FIGURE 2: MgADP and MgATP binding to the wild-type and D129E Fe proteins. Equilibrium column binding of nucleotides to the wild-type or D129E Fe proteins was performed as described under Experimental Procedures. Panel A: MgATP binding to wild-type (■) or D129E (●) Fe proteins. Panel B: MgADP binding to wild-type (□) or D129E (○) Fe proteins. The ratio of the concentration of nucleotide bound to the Fe protein was plotted against the concentration of free nucleotide. In each case, 4 mg of Fe protein was loaded onto the column and collected into one fraction. The data were fit to the Hill equation, $F_b = M_b[S]^n/(K_d + [S]^n)$, where F_b is the fraction of nucleotides bound per Fe protein, M_b is the maximum number of nucleotides bound per Fe protein, [S] is the free nucleotide concentration, and n is the cooperativity factor. For wild-type Fe protein, apparent dissociation constants (K_d) of 128 μM for MgADP and 580 μM for MgATP were determined. For the D129E Fe protein, apparent K_d's of 131 μM for MgADP and 370 μM for MgATP were determined.

However, the D129E Fe protein did show a significant increase in affinity for binding MgATP (apparent K_d for D129E Fe protein of 370 μM compared to 580 μM for the wild-type Fe protein). Fitting of the data presented in Figure 2 to the Hill equation revealed strong cooperativity for both MgATP and MgADP binding to the wild-type Fe protein. The D129E Fe protein showed the same cooperativity in binding MgADP, but little or no (n = 0.8) cooperativity in binding MgATP. In all cases, a maximum of 2 ± 0.1 nucleotides were bound per protein. These results show that the lack of nucleotide hydrolysis by the D129E Fe protein is not the result of the lack of binding of nucleotides and that the change of Asp 129 to Glu has had a positive effect on the affinity for binding MgATP.

MgATP-Induced Conformational Changes in the Fe Protein. Given the preceding results, it was necessary to determine whether the normal nucleotide-induced conformational changes in the Fe protein were affected by altering

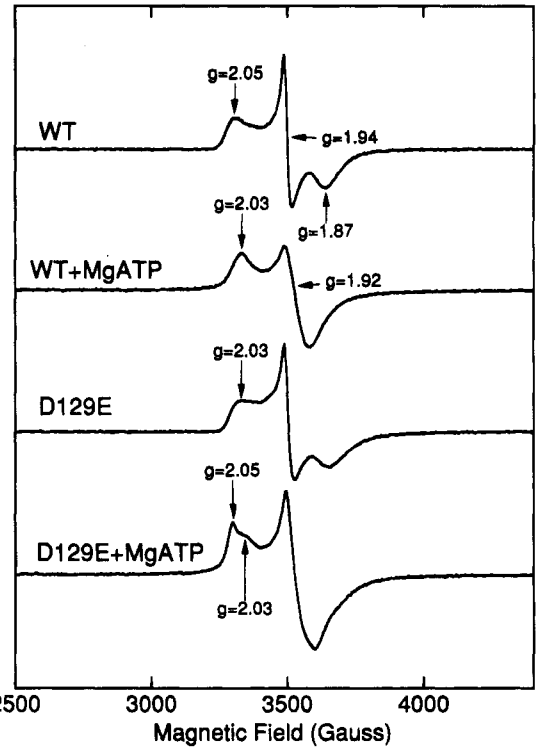

FIGURE 3: EPR spectra of purified wild-type and D129E Fe proteins with and without MgATP. Purified wild-type (WT) and D129E Fe proteins (40 mg mL^{-1}) were prepared as described under Experimental Procedures. All samples contained 0.5 mM dithionite and were prepared and frozen under argon. All spectra were recorded at 12 K, 9.51 GHz, and 0.5 mW of microwave power. Where indicated, MgATP was added as a 10-fold molar excess over protein prior to freezing (+MgATP). Unless noted otherwise, g-values apply to all traces.

Asp 129 to Glu. The location of Asp 129 in a proposed pathway of communication from Asp 125 to Cys 132 made this of particular interest (Wolle et al., 1992). Binding of MgATP to wild-type Fe protein is known to induce conformational changes in the protein that result in changes in the environment of the [4Fe-4S] cluster (Mortenson et al., 1993). A series of techniques can be used to monitor these conformational changes and was applied to the D129E Fe protein.

EPR has been used extensively to monitor both the oxidation state and electronic environment of the [4Fe-4S] cluster in the Fe protein. In the absence of nucleotides, the reduced Fe protein exhibits a rhombic EPR spectrum centered around g = 1.94 (Figure 3). The addition of MgATP to the reduced Fe protein results in a change in the EPR line shape from rhombic to axial (Figure 3). These changes in the line shape have been interpreted to indicate MgATP-induced conformational changes in the environment of the [4Fe-4S] cluster, resulting from nucleotide binding some 19 Å away (Orme-Johnson et al., 1972; Zumft et al., 1972). The EPR spectrum for the reduced D129E Fe protein (Figure 3) was found to be similar, but not identical, to that of the wild-type Fe protein in the absence of nucleotides. Interestingly, in the absence of MgATP, the D129E Fe protein showed a signal at g = 2.03, which is observed for the wild-type Fe protein only in the presence of MgATP. Upon the addition of MgATP to the D129E Fe protein, the EPR line shape appeared to undergo a partial change from the rhombic to the axial line shape. Notably, the D129E Fe protein

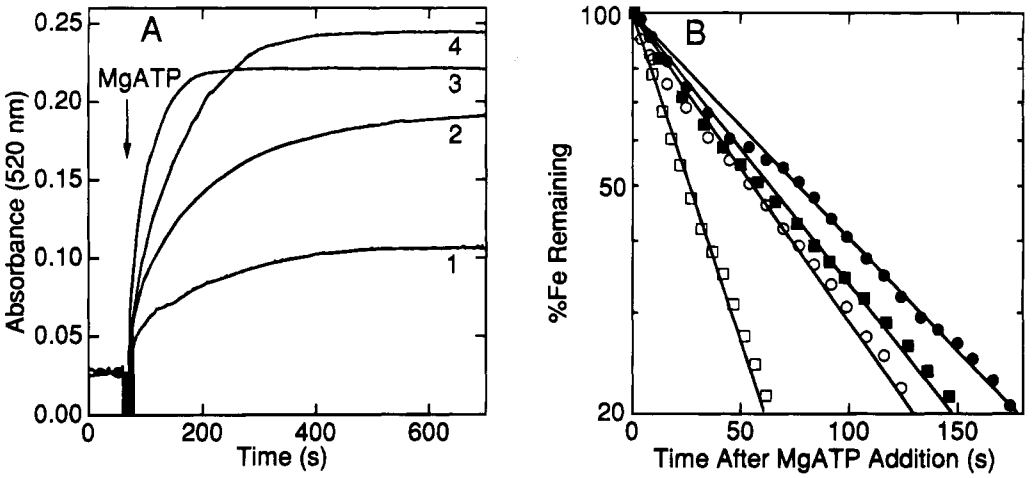

FIGURE 4: Time course for the MgATP-dependent chelation of Fe^{2+} from Fe proteins by α,α′-bipyridyl. Reaction conditions were as described in Experimental Procedures. The absorbance at 520 nm of the Fe^{2+}−α,α′-bipyridyl complex versus time was recorded. For reaction solutions including the MoFe protein, phosphocreatine and creatine phosphokinase were added to prevent the formation of MgADP. Panal A: Wild-type (trace 4) or D129E (trace 3) Fe proteins (435 μg or 6.8 nmol) were added to initiate the reaction. Protection by the MoFe protein was examined by the addition of MoFe protein (836 μg or 3.4 nmol) prior to the addition of wild-type (trace 1) or D129E (trace 2) Fe protein. MgATP was added to a final concentration of 3.9 mM at the time indicated by the arrow. Panel B: The logarithm of the percentage of total releasable iron remaining bound to the Fe protein was plotted versus the time after MgATP addition from the wild-type data in panel A with (●) or without (○) added MoFe protein. Apparent first-order rate constants of 0.008 and 0.012 s^{-1} were determined for the wild-type Fe protein in the presence or absence of MoFe protein, respectively. The logarithm of the percentage of total releasable iron remaining bound to the D129E Fe protein versus time after MgATP addition was plotted from the data in Panel A with (■) or without (□) added MoFe protein. Apparent first-order rate constants of 0.010 and 0.026 s^{-1} were determined for the D129E Fe protein in the presence or absence of MoFe protein, respectively.

contained both $g = 2.05$ and $g = 2.03$ character in the presence of MgATP. Spectra taken at 4 K were also recorded for both wild-type and D129E Fe proteins in the absence or presence of MgATP to confirm the presence of the $S = 3/2$ signal near $g = 4$. These results verify that the D129E Fe protein contains a [4Fe-4S] cluster and suggest that the D129E Fe protein still undergoes nucleotide-induced conformational changes that affect the environment of the [4Fe-4S] cluster. These results further indicate that the longer side chain at position 129 has been adjusted for by the protein backbone and that this adjustment is detected by the cluster. Finally, changing Asp 129 to Glu partially affected the nature of the conformational change upon binding MgATP.

Another sensitive method to monitor the MgATP-induced conformational changes in the Fe protein is the rate of Fe^{2+} chelation from the [4Fe-4S] cluster by α,α′-bipyridyl or bathophenanthrolinedisulfonic acid upon the addition of MgATP. MgATP binding to the Fe protein changes the environment around the [4Fe-4S] cluster such that time-dependent chelation of Fe^{2+} occurs to one of these iron-specific chelators. The rate of Fe^{2+} chelation can be monitored in real time by spectrophotometrically following the formation of the colored Fe^{2+}−chelator complex. Figure 4 (Panel A, traces 3 and 4) illustrates the time course of the MgATP-dependent Fe^{2+} chelation by α,α′-bipyridyl from both wild-type and D129E Fe proteins. The wild-type and D129E Fe proteins both demonstrated similar extents of total Fe^{2+} chelated upon the addition of MgATP. The total amount of Fe released from the wild-type Fe protein was 3.8 ± 0.1 nmol of Fe per nmol of protein, while the D129E Fe protein released 3.6 ± 0.1 nmol of Fe per nmole of Fe protein, confirming that the D129E Fe protein contained a normal complement of Fe in the [4Fe-4S] cluster. No Fe^{2+} chelation was observed for either protein in the absence of MgATP. The rates of Fe^{2+} chelation for wild-type and D129E Fe proteins were, however, found to be quite different. The rates were determined by plotting the logarithm of the percentage of Fe^{2+} remaining bound to the Fe protein against the time after MgATP addition (Figure 4, Panel B). Apparent first-order rate constants of 0.026 s^{-1} and 0.012 s^{-1} for D129E Fe protein and wild-type Fe protein were determined, indicating that the D129E Fe protein released Fe^{2+} at a rate 2.1 times faster than the wild-type Fe protein. These results support the results from EPR suggesting that changing Asp 129 to Glu partially affected MgATP-induced conformational changes in the Fe protein.

Previous studies have shown that the addition of MoFe protein to the Fe^{2+} chelation assay results in a decreased rate of Fe^{2+} chelation (Seefeldt, 1994). This is attributed to the MoFe protein binding to the Fe protein and, thus, protecting the [4Fe-4S] cluster of the Fe protein from chelation. Figure 4 (Panel A, traces 1 and 2) illustrates the effects of adding MoFe protein to the Fe^{2+} chelation assays for wild-type and D129E Fe proteins. The addition of MoFe protein decreased the apparent first-order rate constants for Fe^{2+} chelation for both the wild type (0.008 s^{-1}) and D129E (0.012 s^{-1}) proteins, indicating that both the D129E and wild-type Fe proteins bind to the MoFe protein.

Bathophenanthrolinedisulfonic acid (BPS) has also been used to monitor the MgATP-dependent chelation of Fe^{2+} from Fe protein (Ljones & Burris, 1978). The rate of chelation by BPS has been shown to be significantly faster when compared to α,α′-bipyridyl, suggesting a different mechanism of chelation for the two chelators. We have also examined the rates of Fe^{2+} chelation from wild-type and D129E Fe proteins with BPS as the chelator. Both the wild-type and D129E Fe proteins showed no chelation in the absence of MgATP and a time-dependent chelation of Fe^{2+} after the addition of MgATP. A plot of the logarithm of the percentage of iron remaining bound to the Fe protein against the time after MgATP addition was linear for both

proteins, indicating apparent first-order rates of chelation. The D129E Fe protein, however, demonstrated a 5.3 times faster rate of iron chelation when compared to the wild-type Fe protein (0.122 s^{-1} compared to 0.023 s^{-1}). The total amounts of iron chelated from the wild-type Fe protein (3.3 ± 0.1) and the D129E Fe protein (3.4 ± 0.1) were similar. As determined in the α,α′-bipyridyl chelation assay, the addition of MoFe protein to the BPS chelation assay resulted in a decreased rate of chelation for both wild-type (0.007 s^{-1}) and D129E (0.039 s^{-1}) Fe proteins.

MgADP- and MgATP-Induced Conformational Changes in the Fe Protein. Like MgATP binding to the Fe protein, MgADP binding has also been shown to induce conformational changes in the Fe protein. These changes are clearly different from those induced by MgATP. MgADP will not stimulate the EPR change nor the Fe^{2+} chelation. MgATP or MgADP binding to the Fe protein does, however, result in conformational changes that can be detected as changes in the midpoint reduction potential of the [4Fe-4S] cluster (Watt et al., 1986), changes in the visible circular dichroism (CD) spectrum of the Fe protein (Stephens et al., 1979), or changes in the isotropically shifted protons of the ^1H NMR spectrum of the Fe protein (Meyer et al., 1988). We have examined the D129E Fe protein by microcoulometry, CD spectropolarimetry, and ^1H NMR as sensitive methods to monitor both the MgADP- and MgATP-induced conformational changes in the Fe protein.

The visible region CD spectrum of the oxidized Fe protein provides a sensitive way to detect changes in the environment of the [4Fe-4S] cluster (Stephens et al., 1979). Figure 5A illustrates the visible CD spectra for oxidized wild-type Fe protein in the absence or presence of MgATP or MgADP. Of central importance is the observation that the conformational changes induced by MgADP are distinctly different from those induced by MgATP (L. C. Seefeldt, M. J. Ryle, W. N. Lanzilotta, and G. M. Jensen, unpublished data). The CD spectra for the D129E Fe protein in the absence of nucleotides or in the presence of MgATP or MgADP are also shown in Figure 5 (Panel B). The observation that the D129E Fe protein in the absence of added nucleotides appeared similar to the MgADP-bound state of the wild-type Fe protein was significant. To investigate the possibility that the D129E Fe protein might have a tightly bound MgADP, the protein was denatured with 2.5 M H_2SO_4 and the supernatant was analyzed for MgADP by the HPLC method previously described (Seefeldt & Mortenson, 1993). No MgADP could be detected with a detection limit of 0.02 MgADP (Fe protein)$^{-1}$. The addition of MgADP to the oxidized D129E Fe protein did result in an apparent change in the CD that appeared to be intermediate between the normal wild-type MgADP- and MgATP-bound states. The addition of MgATP to the oxidized D129E Fe protein resulted in a spectrum similar to that observed for the wild-type Fe protein in the presence of MgATP. It is noteworthy that the total ellipticity ($\Delta\epsilon$) of the D129E Fe protein is lower than that observed for the wild-type Fe protein.

Protons near the paramagnetic [4Fe-4S] cluster of the *Clostridium pasteurianum* Fe protein (*Cp2*) have been shown to be isotropically shifted in the ^1H NMR spectrum (Meyer et al., 1988). In addition, the shifts of these protons were sensitive to the binding of both MgATP and MgADP (Meyer et al., 1988). As another sensitive way to monitor the nucleotide-induced changes in Fe protein, we collected ^1H

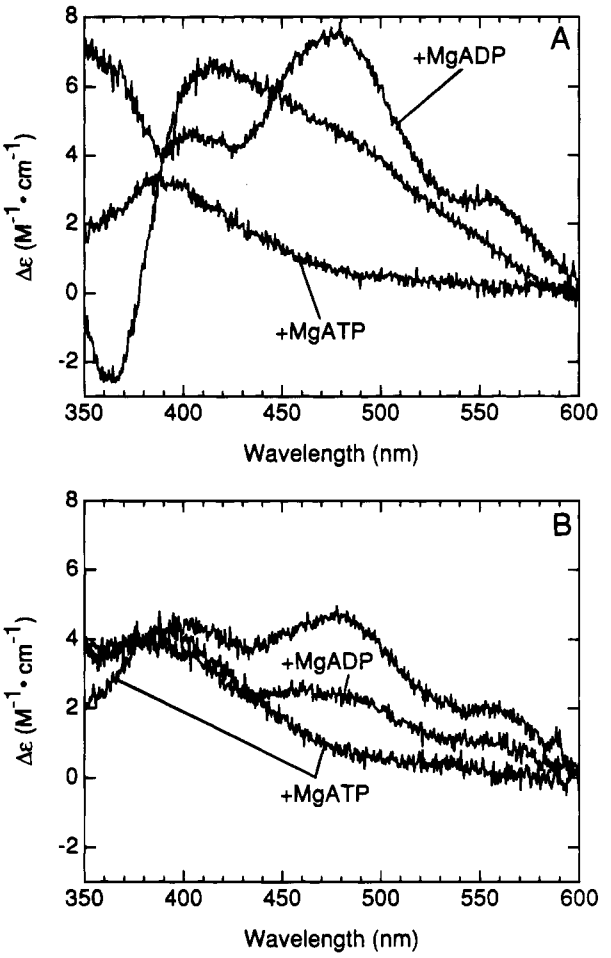

FIGURE 5: Circular dichroism spectra of wild-type and D129E Fe proteins with and without nucleotides. Visible region circular dichroism (CD) spectra of the oxidized wild-type and D129E Fe proteins were recorded as described under Experimental Procedures. Panel A: CD spectra for the oxidized wild-type Fe protein in the absence of nucleotides, in the presence of 1 mM MgATP (+MgATP), and in the presence of 1 mM MgADP (+MgADP). Panel B: CD spectra of D129E Fe protein in the absence of nucleotides, in the presence of 1 mM MgATP (+MgATP), and in the presence of 1 mM MgADP (+MgADP). All spectra were baseline subtracted.

NMR data for both the wild-type and D129E Fe proteins from *A. vinelandii* (*Av2*). Figure 6A illustrates the position of four isotropically shifted proton signals observed for both the wild-type and D129E Fe proteins. Both Fe proteins demonstrated two sharp signals and two broad signals over a spectral range of 10−60 ppm. The chemical shifts for each signal were different for wild-type and D129E Fe protein and somewhat different from those reported for the Fe proteins from *C. pasteurianum* (Table 1). Upon the addition of MgATP or MgADP to the wild-type Fe protein (Figure 6B,C), each signal showed different chemical shifts arising from different interactions with the paramagnetic cluster. Consistent with the EPR and CD data, the ^1H NMR spectrum of the D129E Fe protein reveals conformational changes in the Fe protein resulting from the amino acid change and changes in both the MgADP- and MgATP-induced states of the cluster environment.

Changes in the Midpoint Potential of the [4Fe-4S] Cluster of Fe Proteins. Both MgATP and MgADP binding to the Fe protein has been shown to reduce the midpoint potential of the $[4Fe\text{-}4S]^{1+/2+}$ couple from −290 to −430 mV. Figure

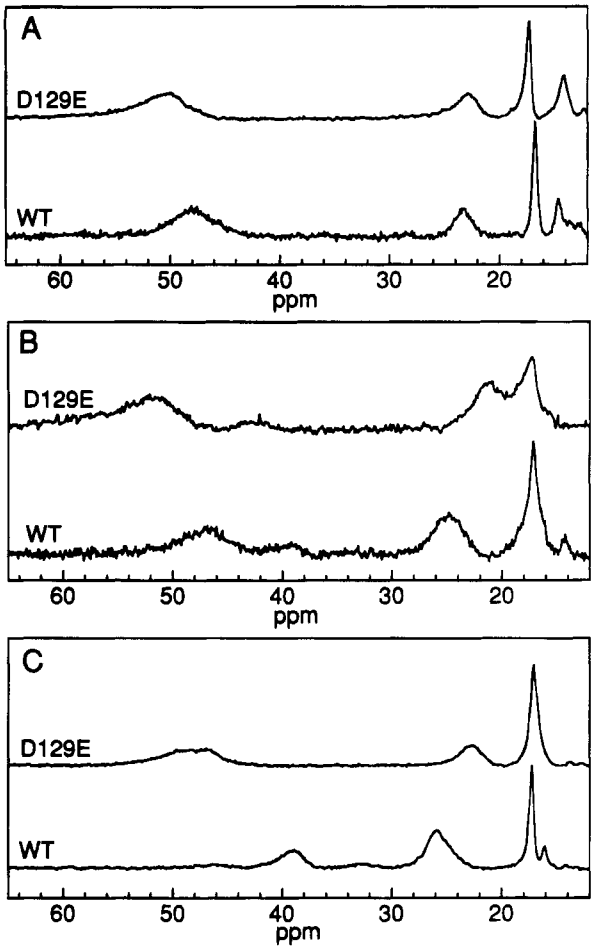

FIGURE 6: ^{1}H NMR spectra of wild-type and D129E Fe proteins. Reduced Fe proteins were prepared as described in the Experimental Procedures. Panel A: Isotropically shifted ^{1}H NMR signals observed for wild-type (WT) and D129E (D129E) Fe proteins. Panel B: Isotropically shifted ^{1}H NMR signals observed for wild-type (WT) and D129E (D129E) Fe proteins in the presence of 5 mM MgATP. Panel C: Isotropically shifted signals observed for wild-type (WT) and D129E (D129E) Fe proteins in the presence of 5 mM MgADP.

Table 1: Isotropically Shifted ^{1}H NMR Signals of Reduced Fe Proteins

chemical shift[a] (ppm)								
no nucleotides			+MgATP			+MgADP		
Cp2	*Av2*	D129E *Av2*	*Cp2*	*Av2*	D129E *Av2*	*Cp2*	*Av2*	D129E *Av2*
46.9			42.0	47.0	51.5	42.0	46.1	47.5
45.1	48.5	49.9		38.7	42.8	39.1	38.8	
43.1							32.5	
24.9	23.2	22.8	25.2	25.9		25.6	25.8	
17.4		17.2	21.7	24.6	20.9	22.4		22.8
16.5	16.5		16.8	17.1	17.2	16.1	17.2	17.0
15.5	14.4	14.0					15.9	

[a] The chemical shifts are given in parts per million at 313 K for the D129E and wild-type *A. vinelandii* Fe proteins (*Av2*) and are referenced to the water proton signals at 4.7 ppm. The signals observed for the *Av* Fe proteins are compared to those observed for the *C. pasteurianum* Fe protein (*Cp2*) (Meyer et al., 1988).

7A shows microcoulometric determination of the midpoint reduction potentials for wild-type Fe protein. A similar experiment was performed with the D129E Fe protein and is illustrated in Figure 7B. Midpoint reduction potentials for the D129E Fe protein were found to be −300 mV in the absence of nucleotides, −430 mV in the presence of MgATP, and −440 mV in the presence of MgADP. These results were within experimental error of the potentials determined for wild-type Fe protein. These results reveal that, despite apparent differences in the environment of the [4Fe-4S] cluster of the D129E Fe protein detected by EPR, CD, and ^{1}H NMR, the midpoint reduction potentials of the D129E Fe protein, both in the absence and presence of nucleotides, are unaffected. It is possible that the potential of the D129E Fe protein has changed by less than the 20 mV resolution of the method.

Binding of the D129E Fe Protein to the MoFe Protein. Examination of the affinity of the D129E Fe protein for docking to the MoFe protein was potentially important to explain why no substrate reduction or MgATP hydrolysis was observed for the D129E Fe protein−MoFe protein complex. The MoFe protein protection of Fe^{2+} chelation from the D129E Fe protein observed earlier suggested that the D129E Fe protein could still bind to the MoFe protein. To further quantify the affinity of the D129E Fe protein for binding to the MoFe protein, we employed a competition binding activity assay. Earlier we demonstrated that the D129E Fe protein would not support acetylene reduction activity when combined with the MoFe protein. Thus, it was possible to include increasing concentrations of D129E Fe protein in a normal wild-type Fe protein−MoFe protein assay to determine the effects on the substrate reduction rates. The assumption was that if the D129E Fe protein could bind to the MoFe protein to form an inactive complex, then a decrease in the substrate reduction rates catalyzed by the wild-type Fe protein−MoFe protein complex would be observed. If the D129E Fe protein did not bind to the MoFe protein, then increasing D129E Fe protein concentrations in a normal wild-type Fe protein−MoFe protein assay would have no effect on the substrate reduction rates. Figure 8 illustrates the effects of increasing D129E Fe protein concentrations on the acetylene reduction activity catalyzed by wild-type Fe protein and MoFe protein, demonstrating a clear decrease in acetylene reduction activity with the addition of increasing D129E Fe protein. The data in Figure 8 were fit to the Hill equation, where it was found that 50% inhibition of activity occurred at a 1:1 ratio of D129E Fe protein to wild-type Fe protein. This suggests that the D129E and wild-type Fe proteins are competing equally for binding to the MoFe protein and, therefore, that the D129E Fe protein binds to the MoFe protein with normal affinity. It is interesting to note that the Hill equation fit suggested cooperativity in the binding of Fe protein to the MoFe protein, with two sites suggested. This is consistent with the current model, which suggests that the MoFe protein has two Fe protein-binding sites (Kim et al., 1993). A K15R Fe protein, which does not bind to the MoFe protein (Ryle et al., 1995), was also used in this experiment as a negative control and was found to have no effect on the wild-type activity, even up to a ratio of 2.4 K15R Fe proteins to 1 wild-type Fe protein. Therefore, it was concluded that the D129E Fe protein could still bind to the MoFe protein, but could not support MgATP hydrolysis or electron transfer to the MoFe protein.

DISCUSSION

MgATP binding and hydrolysis are of central importance in the substrate reduction mechanism of nitrogenase. The

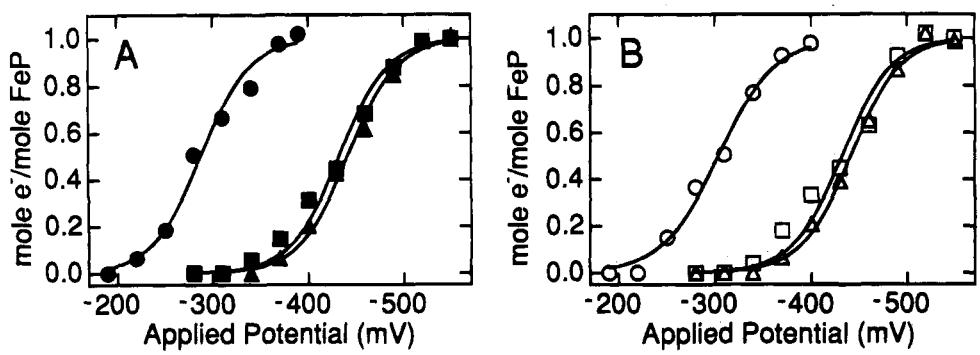

FIGURE 7: Reduction curves for the wild-type and D129E Fe proteins with and without nucleotides. Coulometric electrochemical reductions of oxidized wild-type or D129E Fe proteins were performed as outlined in Experimental Procedures. Panel A: Reduction curves for wild-type Fe protein in the absence of nucleotides (●), in the presence of 3 mM MgATP (■), or in the presence of 3 mM MgADP (▲). Midpoint potentials were determined to be −290, −430, and −440 mV, respectively. Panel B: Reduction curves for the D129E Fe protein in the absence of nucleotides (○), in the presence of MgATP (□), or in the presence of MgADP (△). Midpoint potentials were determined to be −300, −430, and −440 mV, respectively. All midpoint potentials are reported relative to the standard hydrogen electrode (SHE).

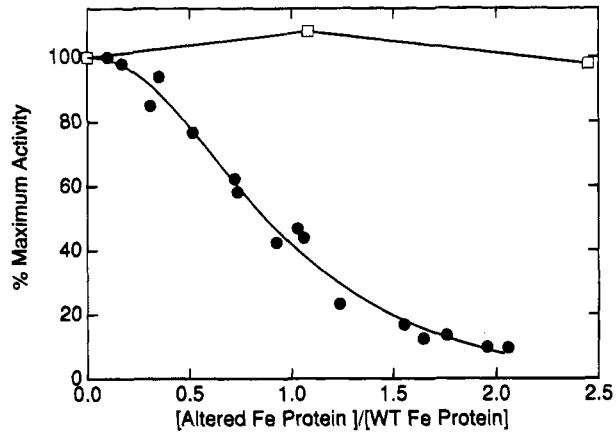

FIGURE 8: Inhibition of wild-type nitrogenase acetylene reduction activity by D129E Fe protein. Acetylene reduction assays were performed as described in the Experimental Procedures. 216 μg (0.9 nmol) of wild-type MoFe protein was added to each assay vial. Increasing amounts (from 0 to 240 μg) of D129E (●) or K15R Fe protein (□) were added to each vial. The reaction was initiated by the addition of 115 μg (1.8 nmol) of wild-type Fe protein. The percentage of the maximum acetylene reduction activity (nanomoles of ethylene produced minute^{-1}) was plotted against the ratio of altered Fe protein (D129E or K15R) to wild-type Fe protein. The maximum activity in the absence of added D129E Fe protein was 2030 nmol of ethylene min^{-1} mg^{-1}. The data for D129E Fe protein were fit to the inverse Hill equation, $(1/v) = (K_m + [S]^n)/(V_{max}[S]^n)$, where n was found to be 2.2, and 50% activity remaining was observed at a ratio of 0.9 (D129E Fe protein/wild type Fe protein).

results presented in this work provide evidence of a central role for Asp 129 of *A. vinelandii* nitrogenase Fe protein in MgATP binding, nucleotide-induced protein conformational changes, and possibly directly in MgATP hydrolysis.

MgATP Binding. The binding of MgATP to the Fe protein is a necessary first step in the mechanism of substrate reduction. We have recently shown that Lys 15 of the *A. vinelandii* Fe protein plays a central role in the binding of both MgATP and MgADP to the Fe protein (Ryle et al., 1995), probably through interactions with the β- and γ-phosphate portions of bound MgATP. Ser 16 has been suggested to interact with the bound Mg^{2+}, which is expected to be bound to the β- and γ-phosphates of ATP (Seefeldt & Mortenson, 1993). The location of Asp 129 near Lys 15 and Ser 16 (Figure 1) clearly suggested a role for this residue in binding the phosphate portion of nucleotides. The negatively charged carboxylate side chain of Asp 129 would not be expected to interact directly with the negatively charged phosphates, but rather might be expected to interact with either the Mg^{2+} or a bound water. The interaction with Mg^{2+} seems less likely given the location of Asp 129 some distance away from Ser 16, a likely ligand to the Mg^{2+}. Instead, interaction with a bound water seems most likely. Interestingly, the longer side chain of Glu at position 129 resulted in an increased affinity for MgATP, while there was no effect on the affinity for MgADP. This would suggest that if Asp 129 is interacting with a bound water, this water is interacting with the γ-phosphate portion of ATP and not with the α- or β-phosphate portions of ADP. The location of a water molecule bound near Asp 129 would be consistent with the need for a water molecule for nucleophilic attack on the γ-phosphate of ATP for hydrolysis.

Nucleotide-Induced Protein Conformational Changes. Upon binding to the Fe protein, both MgADP and MgATP induce conformational changes in the Fe protein that are clearly essential for Fe protein docking to the MoFe protein, electron transfer, and substrate reduction. The mechanism of these conformational changes in the Fe protein appears to be complex. It is clear that these protein conformational changes are reflected as changes in the environment of the [4Fe-4S] cluster, which is approximately 19 Å away from the phosphate site. Previous work has suggested that at least one mechanism for communication between the nucleotide-binding site and the [4Fe-4S] cluster could be mediated by movement in the protein backbone between Asp 125 and Cys 132 (Wolle et al., 1992). Asp 125 is located in the phosphate-binding site of the Fe protein, opposite Lys 15. Cys 132, only seven residues away, provides two of four ligands to the [4Fe-4S] cluster. It seems likely that, in the absence of nucleotides, Lys 15 and Asp 125 form a salt bridge, which is broken upon the binding of the phosphate portion of a nucleotide (Georgiadis et al., 1992; Ryle et al., 1995). With nucleotide bound, Lys 15 is expected to interact with the negatively charged phosphates and Asp 125 with the Mg^{2+}. The movement of Asp 125 might be expected to move the connection to the cluster ligand, changing the environment of the [4Fe-4S] cluster. Recently, it has been found that changing Lys 15 to Arg appears to "lock" the phosphate-binding site by the formation of a stronger bridge to Asp 125, so that neither MgATP nor MgADP could bind (Ryle et al., 1995). All nucleotide-induced conformational changes were blocked. Likewise, changing Asp 125 to Glu

was found to change the communication between the phosphate site and the [4Fe-4S] cluster (Wolle et al., 1992).

The location of Asp 129 between Asp 125 and Cys 132 and in the phosphate-binding site clearly suggested a function in the communication between the phosphate site and the cluster. The results presented in this work from the EPR, chelation rates, CD, and isotropically shifted ^{1}H NMR of the D129E Fe protein support such a role for Asp 129. Both EPR and CD suggested that, by lengthening the carboxylate side chain at residue 129 (D129E), a partial change in the cluster has occurred that mimics the binding of nucleotides. It is possible that lengthening the position of the carboxylate has pushed the connection to Cys 132 in a way similar to that caused by the nucleotide phosphate binding. The faster rate of iron chelation after MgATP binding also supports this mechanism. It seems possible that, upon binding MgATP, the longer side chain on Glu 129 results in a more pronounced change in the connection to the cluster and, thus, a more dramatic change in the cluster, resulting in an even faster rate of chelation. The EPR, CD, ^{1}H NMR, and chelation experiments suggest that while the nucleotide-induced conformational changes are still occurring, the extent of these nucleotide-induced conformational changes has been affected.

MgATP Hydrolysis. A significant finding of the present work is that the D129E Fe protein still binds to the MoFe protein with normal affinity. Several important comments can be made from this observation. It is important to note that the D129E Fe protein can still bind MgATP, still undergo nucleotide-induced conformational changes (including the lowering of the redox potential of the cluster), and dock with the MoFe protein, but it cannot support MgATP hydrolysis, electron transfer to the MoFe protein, or substrate reduction. This provides evidence that the function of MgATP hydrolysis in electron transfer from the Fe protein to the MoFe protein is not simply to lower the midpoint potential of the Fe protein cluster, and it further supports earlier proposals that MgATP hydrolysis precedes electron transfer from the Fe protein to the MoFe protein (Thorneley & Lowe, 1985).

The lack of MgATP hydrolysis by the D129E Fe protein−MoFe protein complex could be explained if Asp 129 participated in the mechanism of hydrolysis of MgATP. Given the location of Asp 129 near the γ-phosphate of bound MgATP, it is reasonable to assume that Asp 129 could be bound to a water molecule poised for activation of nucleophilic attack on the γ-phosphate. Thus, by changing Asp 129 to Glu, it might be expected that this critical water molecule is out of place for activation and hydrolysis. While the D129E Fe protein binds MgATP, undergoes the necessary conformational changes, and binds to the MoFe protein, it is unable to hydrolyze MgATP and, thus, is unable to transfer an electron to the MoFe protein.

This proposed function of Asp 129 in the nitrogenase Fe protein is supported by analyses of homologous residues in several other nucleotide-hydrolyzing enzymes for which high-resolution X-ray structures are known, often with bound nucleotides or nucleotide analogs. Models for the GTP- and ATP-binding sites of EF-Tu (Hwang & Miller, 1987; Sprinzl, 1994), Ras p21 (Feuerstein et al., 1989; Langen et al., 1992), G-proteins (Coleman et al., 1994), transducin-α (Noel et al., 1993), F_1-ATPase (Abrahams et al., 1994), and recA (Story & Steitz, 1992) have been proposed and can be compared to that proposed for nitrogenase Fe protein. X-ray structures for EF-Tu, which binds and hydrolyzes MgGTP, with bound nucleotides has suggested a model in which Asp 87 and His 85 act as general bases in the activation of a water for hydrolysis of the GTP (Sprinzl, 1994). Much like nitrogenase Fe protein, the binding of another protein to EF-Tu, namely, GAP, activates EF-Tu for GTP hydrolysis. It is possible that Asp 87 in EF-Tu is moved into place for hydrolysis (Sprinzl, 1994). A similar model was proposed for the GTPase Ras p21(Langen et al., 1992). It was suggested that Gln 61 might act as a general base for the activation of a water for hydrolysis, but recent results from site-directed mutagenesis have revealed that Gln 61 is unlikely to function as a general base (Schweins et al., 1994). One proposal suggests that GTP acts as its own base for the activation of a water for hydrolysis (Schweins et al., 1994). It has been suggested that Glu 203 in the protein transducin-α might function as a general base for the activation of a water for hydrolysis of GTP (Noel et al., 1993). Likewise, Glu 188 of the β-subunit of F_1-ATPase (Abrahams et al., 1994) and Glu 96 (Story & Steitz, 1992) of the recA protein have been proposed to function as general bases for the activation of a bound water for hydrolysis. The results presented in this work suggest that Asp 129 of the nitrogenase Fe protein might function in a manner similar to the Asp or Glu residues in other GTPase or ATPase enzymes to either coordinate or activate a water molecule for hydrolysis.

How then does MoFe protein binding to the Fe protein stimulate MgATP hydrolysis? Our current model would suggest that Asp 129 might bind the water molecule that is used for hydrolysis of the γ-phosphate of MgATP. Upon binding to the MoFe protein, a movement in the chain from Cys 132 (the cluster ligand and near the site of MoFe protein binding) to Asp 129 might occur, so that a proton is abstracted from the bound water and the resulting hydroxide undergoes nucleophilic attack on the γ-phosphate, resulting in hydrolysis. Another possible mechanism is that while Asp 129 ligates the bound water, the nearby Asp 39 is moved into place for abstraction of a proton from the water. Asp 39 is near the location of Asp 129 in the X-ray structure of the Fe protein, but is somewhat out of place for coordination of the expected location for the bound water. It is possible that, upon binding of the MoFe protein, Asp 39 is moved into position to activate the bound water. Such a mechanism is supported by the recent observation that Fe protein residues 59−67 are involved in binding to the MoFe protein (Peters et al., 1994). Thus, it seems reasonable that MoFe protein binding to residues in this region of the Fe protein could be mediated through protein backbone changes to Asp 39, moving this residue into position to activate a water. The possible function of Asp 39 in the Fe protein is currently under investigation.

ACKNOWLEDGMENT

The authors thank Drs. Leonard E. Mortenson and T. Vance Morgan for helpful discussions and Drs. Gerard M. Jensen and David B. Goodin of the Scripps Research Institute for assistance with EPR and CD. We also thank Dr. Gerald D. Watt of Brigham Young University for assistance with electrochemistry and Dr. Richard Holz for assistance with NMR.

REFERENCES

Abrahams, J. P., Leslie, A. G. W., Lutter, R., & Walker, J. E. (1994) *Nature 370,* 621−628.

Anderson, G. L., & Howard, J. B. (1984) *Biochemistry 23,* 2118−2122.

Bolin, J. T., Ronco, A. E., Mortenson, L. E., Morgan, T. V., Williamson, M., & Xuong, N. H. (1990) in *Nitrogen Fixation: Achievements and Objectives* (Gresshoff, P. M., Roth, L. E., Stacey, G., & Newton, W. E., Eds.) pp 117−122, Chapman and Hall, New York.

Bordo, D., & Argos, P. (1991) *J. Mol. Biol. 217,* 721−729.

Burris, R. H. (1991) *J. Biol. Chem. 266,* 9339−9342.

Chromy, V., Fischer, J., & Kulhanek, V. (1974) *Clin. Chem. 20,* 1362−1363.

Coleman, D. E., Berghuis, A. M., Lee, E., Linder, M. E., Gilman, A. G., & Sprang, S. R. (1994) *Science 265,* 1405−1412.

Dean, D. R., Bolin, J. T., & Zheng, L. (1993) *J. Bacteriol. 175,* 6737−6744.

Feuerstein, J., Goody, R. S., & Webb, M. R. (1989) *J. Biol. Chem. 264,* 6188−6190.

Georgiadis, M. M., Komiya, H., Chakrabarti, P., Woo, D., Kornuc, J. J., & Rees, D. C. (1992) *Science 257,* 1653−1659.

Hageman, R. V., & Burris, R. H. (1978) *Proc. Natl. Acad. Sci. U.S.A. 75,* 2699−2702.

Hochmann, J., & Kellerhals, H. J. (1990) *Magn. Reson. 28,* 23−29.

Howard, J. B., & Rees, D. C. (1994) *Annu. Rev. Biochem. 63,* 235−264.

Hwang, Y. W., & Miller, D. L. (1987) *J. Biol. Chem. 262,* 13081−13085.

Jacobson, M. R., Brigle, K. E., Bennett, L. T., Setterquist, R. A., Wilson, M. S., Cash, V. L., Beynon, J., Newton, W. E., & Dean, D. R. (1989a) *J. Bacteriol. 171,* 1017−1027.

Jacobson, M. R., Cash, V. L., Weiss, M. C., Laird, N. F., Newton, W. E., & Dean, D. R. (1989b) *Mol. Gen. Genet. 219,* 49−57.

Kim, J., & Rees, D. C. (1992) *Nature 360,* 553−560.

Kim, J., & Rees, D. C. (1994) *Biochemistry 33,* 389−397.

Kim, J., Woo, D., & Rees, D. C. (1993) *Biochemistry 32,* 7104−7115.

Langen, R., Schweins, T., & Warshel, A. (1992) *Biochemistry 31,* 8691−8696.

Ljones, T., & Burris, R. H. (1978) *Biochemistry 17,* 1866−1872.

Meyer, J., Gaillard, J., & Moulis, J. M. (1988) *Biochemistry 27,* 6150−6156.

Mortenson, L. E., Seefeldt, L. C., Morgan, T. V., & Bolin, J. (1993) *Adv. Enzymol. 67,* 299−373.

Noel, J. P., Hamm, H. E., & Sigler, P. B. (1993) *Nature 366,* 654−662.

Normand, P., & Bousquet, J. (1989) *J. Mol. Evol. 29,* 436−447.

Orme-Johnson, W. H., Hamilton, W. D., Jones, T. L., Tso, M. Y. W., Burris, R. H., Shah, V. K., & Brill, W. J. (1972) *Proc. Natl. Acad. Sci. U.S.A. 69,* 3142−3145.

Peters, J. W., Fisher, K., & Dean, D. R. (1994) *J. Biol. Chem. 269,* 28076−28083.

Ryle, M. J., Lanzilotta, W. N., Mortenson, L. E., Watt, G. D., & Seefeldt, L. C. (1995) *J. Biol. Chem. 270,* 13112−13117.

Schweins, T., Langen, R., & Warshel, A. (1994) *Struct. Biol. 1,* 476−484.

Seefeldt, L. C. (1994) *Protein Sci. 3,* 2073−2081.

Seefeldt, L. C., & Mortenson, L. E. (1993) *Protein Sci. 2,* 93−102.

Seefeldt, L. C., & Ensign, S. A. (1994) *Anal. Biochem. 221,* 379−386.

Seefeldt, L. C., Morgan, T. V., Dean, D. R., & Mortenson, L. E. (1992) *J. Biol. Chem. 267,* 6680−6688.

Smith, B. E., & Eady, R. R. (1992) *Eur. J. Biochem. 205,* 1−15.

Sprinzl, M. (1994) *Trends Biochem. Sci. 19,* 245−250.

Stephens, P. J., McKenna, C. E., Smith, B. E., Nguyen, H. T., McKenna, M. C., Thomson, A. J., Devlin, F., & Jones, J. B. (1979) *Proc. Natl. Acad. Sci. U.S.A. 76,* 2585−2589.

Story, R. M., & Steitz, T. A. (1992) *Nature 355,* 374−376.

Thorneley, R. N. F., & Lowe, D. J. (1985) in *Molybdenum Enzymes* (Spiro, T. G., Ed.) pp 221−284, Wiley, New York.

Walker, G. A., & Mortenson, L. E. (1974) *Biochemistry 13,* 2382−2388.

Watt, G. D., Wang, Z. C., & Knotts, R. R. (1986) *Biochemistry 25,* 8156−8162.

Wolle, D., Dean, D. R., & Howard, J. B. (1992) *Science 258,* 992−995.

Yates, M. G. (1991) in *Biological Nitrogen Fixation* (Stacey, G., Burris, R. H., & Evans, H. J., Eds.) pp 685−735, Chapman and Hall, New York.

Zumft, W. G., Cretney, W. C., Huang, T. C., Mortenson, L. E., & Palmer, G. (1972) *Biochem. Biophys. Res. Commun. 48,* 1525−1532.

BI951046L